

SCIENTIFIC REPORTS



OPEN

ACVR2B/Fc counteracts chemotherapy-induced loss of muscle and bone mass

Rafael Barreto¹, Yukiko Kitase^{2,3}, Tsutomu Matsumoto^{2,3}, Fabrizio Pin^{2,3}, Kyra C. Colston⁴, Katherine E. Couch⁴, Thomas M. O'Connell^{3,5,6,7}, Marion E. Couch^{3,5,6,7}, Lynda F. Bonewald^{2,3,6,7} & Andrea Bonetto^{1,2,3,5,6,7}

Chemotherapy promotes the development of cachexia, a debilitating condition characterized by muscle and fat loss. ACVR2B/Fc, an inhibitor of the Activin Receptor 2B signaling, has been shown to preserve muscle mass and prolong survival in tumor hosts, and to increase bone mass in models of osteogenesis imperfecta and muscular dystrophy. We compared the effects of ACVR2B/Fc on muscle and bone mass in mice exposed to Folfiri. In addition to impairing muscle mass and function, Folfiri had severe negative effects on bone, as shown by reduced trabecular bone volume fraction (BV/TV), thickness (Tb.Th), number (Tb.N), connectivity density (Conn.Dn), and by increased separation (Tb.Sp) in trabecular bone of the femur and vertebra. ACVR2B/Fc prevented the loss of muscle mass and strength, and the loss of trabecular bone in femurs and vertebrae following Folfiri administration. Neither Folfiri nor ACVR2B/Fc had effects on femoral cortical bone, as shown by unchanged cortical bone volume fraction (Ct.BV/TV), thickness (Ct.Th) and porosity. Our results suggest that Folfiri is responsible for concomitant muscle and bone degeneration, and that ACVR2B/Fc prevents these derangements. Future studies are required to determine if the same protective effects are observed in combination with other anticancer regimens or in the presence of cancer.

It is estimated that 1.7 million new cases of cancer will be diagnosed in the United States this year, and up to 600,000 people will die from the disease¹. Up to 80% of all advanced cancer patients will present with signs of cachexia. This condition is characterized by depletion of skeletal muscle mass and adipose tissue, persistent muscle fatigue, anorexia, increased inflammatory state, worsened quality of life and overall shorter survival^{2–6}. Experimental evidence suggests that bone loss, a disorder that primarily occurs concurrent to the formation of distal metastases in lung carcinomas, prostate and breast cancer^{7,8}, is also a primary feature accompanying the development of a severe cachectic phenotype. This phenotype has been described in myeloma, colorectal and pancreatic cancers and burn-induced cachexia^{9–13}.

Notably, musculoskeletal degenerations, often culminating with extensive muscle and bone loss, are the most common and most distressing symptoms associated with the development of cancer, as well as with its management and treatment^{7,14–16}. We recently showed that anti-cancer regimens routinely used for the therapy of solid tumors, such as Folfiri (a combination of 5-fluorouracil, leucovorin and irinotecan), contribute to the development of cachexia and promote the loss of muscle tissue and muscle strength¹⁷. Similarly, chemo- and radiotherapy have been reported to play a role in bone loss by directly targeting bone mass^{18,19}, promoting indirect systemic effects^{20,21}, affecting bone remodeling^{22,23} or causing myelosuppression^{24,25}.

The identification of muscle- and bone-derived factors for the generation of new treatment strategies is far from being accomplished. No effective therapy is currently approved for the concurrent treatment of muscle wasting and osteoporosis associated with cancer growth or anti-cancer therapies. It is estimated that cachexia

¹Department of Surgery, Indiana University School of Medicine, Indianapolis, IN, 46202, USA. ²Department of Anatomy and Cell Biology, Indiana University School of Medicine, Indianapolis, IN, 46202, USA. ³Indiana Center for Musculoskeletal Health, Indiana University School of Medicine, Indianapolis, IN, 46202, USA. ⁴Indianapolis Project STEM, Indiana University School of Medicine, Indianapolis, IN, 46202, USA. ⁵Department of Otolaryngology - Head and Neck Surgery, Indiana University School of Medicine, Indianapolis, IN, 46202, USA. ⁶Simon Cancer Center, Indiana University School of Medicine, Indianapolis, IN, 46202, USA. ⁷IUPUI Center for Cachexia Research Innovation and Therapy, Indiana University School of Medicine, Indianapolis, IN, 46202, USA. Correspondence and requests for materials should be addressed to A.B. (email: abonetto@iu.edu)

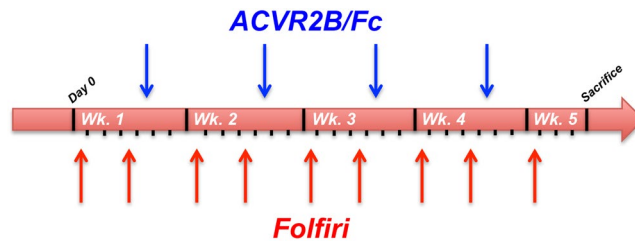


Figure 1. Experimental plan. Schematic representation of the experimental model and dosing schedules. The black ticks indicate the days, the blue arrows the day of ACVR2B/Fc treatment and the red arrows the day of Folfiri treatment. Wk. = week.

ultimately accounts for 25–30% of all cancer-related deaths each year, thereby representing an important clinical problem^{4,26}. While no therapies are available for the treatment of cancer-associated muscle wasting, only a few compounds, e.g. bisphosphonates and denosumab, are approved for the prevention of bone loss in combination with cancer or chemotherapy, although issues related to limited efficacy and long-term side effects have been reported in some cases²⁷. Similarly, other compounds, such as the parathyroid hormone (PTH) and PTH-related protein (PTHrP) peptides, are currently being tested, while their limited applicability in association with cancer still needs to be clarified^{28–30}.

In an attempt to isolate novel compounds endowed with muscle- and bone-protective properties, inhibition of the activin receptor 2B (ACVR2B) signaling was shown to enhance muscle mass, increase overall survival in experimental cancer cachexia^{31,32}, and to ameliorate the dystrophic phenotype in *mdx* mice³³. We and others showed that ACVR2B/Fc, a soluble ACVR2B fusion protein and inhibitor of receptor downstream signaling³⁴, potently counteracts the Folfiri-associated myofiber atrophy in C2C12 cultures¹⁷ and prevents muscle wasting in combination with doxorubicin³⁵ or cisplatin³⁶. Administration of ACVR2B/Fc was also shown to concurrently prevent bone loss in a mouse model of osteogenesis imperfecta³⁷ and in dystrophic mice³⁸.

We hypothesized that inhibition of the activin signaling by means of ACVR2B/Fc could represent a novel strategy to treat musculoskeletal conditions associated with chemotherapy treatments, thereby improving both muscle and bone properties. To test our hypothesis, we treated CD2F1 mice with Folfiri, ACVR2B/Fc, or a combination of both for up to five weeks, and the effects on muscle size and strength were evaluated. In addition to muscle mass and function, we assessed the effects on bone mass, specifically trabecular bone volume fraction (BV/TV), thickness (Tb.Th), number (Tb.N), connectivity density (Conn.Dn), and trabecular separation (Tb.Sp) in trabecular bone of the femur and vertebra. In order to better understand the consequence of ACVR2B/Fc administration to healthy animals and mice treated with Folfiri, we also assessed the circulating levels of IL-6 and activin A, previously reported to play a major role in promoting cachexia and in the regulation of muscle and bone mass.

Results

ACVR2B/Fc preserves body weight in animals exposed to Folfiri. In order to test the use of ACVR2B/Fc for the prevention of chemotherapy-derived loss of muscle mass and muscle strength, we took advantage of a previously characterized experimental model¹⁷. CD2F1 male mice (8 week-old) received Folfiri (twice/weekly, i.p.), with or without ACVR2B/Fc (once/weekly, i.p.), for up to 5 weeks (Fig. 1). Consistent with our previous data^{17,39}, after an initial lag phase, the animals that were treated with Folfiri lost about 20% of their body weight (-5.21 ± 0.32 g; $p < 0.001$ vs. Vehicle). The animals receiving the combination of Folfiri + ACVR2B/Fc displayed a substantial preservation of body mass (2.36 ± 1.14 g; $p < 0.001$ vs. Folfiri) when compared to the Vehicle-treated animals (2.13 ± 0.71 g) (Fig. 2A,B). The animals administered the ACVR2B/Fc alone showed a marked increase in body weight (5.73 ± 0.32 g; $p < 0.001$ vs. Vehicle), in line with previous findings^{31,34} (Fig. 2A,B). The assessment of the body composition performed by means of EchoMRI showed a precocious loss of fat tissue in the animals receiving Folfiri that ultimately was only partially preserved by ACVR2B/Fc treatment (Fig. 3). In line with the body weight data shown in Fig. 2, the administration of ACVR2B/Fc promoted general muscle hypertrophy and completely counteracted the loss of lean tissue as mediated by Folfiri treatment (Fig. 3).

Administration of ACVR2B/Fc protects muscle mass in Folfiri-treated mice. In line with our previous studies^{17,39}, chronic administration of Folfiri to male CD2F1 mice led to marked loss of muscle tissue compared to the Vehicle-treated animals. Specifically, the chemotherapy-induced muscle wasting was consistent with markedly reduced size of tibialis anterior (-22% ; $p < 0.001$), gastrocnemius (-22% ; $p < 0.001$), quadriceps (-26% ; $p < 0.001$) and heart (-13% ; $p < 0.001$) (Fig. 4). To better understand whether gender-specific effects could affect the chemotherapy-associated muscle toxicity, we tested Folfiri also in female CD2F1 mice. Interestingly, the administration of the same chemotherapy regimen to female mice was promoting the occurrence of significant depletion of muscle mass (e.g. gastrocnemius: -13% vs. Vehicle; $p < 0.05$) and reduced muscle strength (-7% vs. Vehicle; $p < 0.05$) (Supplementary Figure S1). However, the chemotherapy-associated effects seemed to be less pronounced in the females, showing moderate loss of muscle mass and muscle weakness with respect to the males. Hence, we investigated the muscle-protective properties of ACVR2B/Fc in the male mice only, due to their apparently enhanced susceptibility to the effects of anti-cancer agents. ACVR2B/Fc was able to promote muscle hypertrophy, as shown by increased quadriceps size ($+36\%$ vs. Vehicle; $p < 0.001$), and to completely reverse the Folfiri-induced muscle atrophy ($+13\%$ vs. Folfiri; $p < 0.001$) (Fig. 4). ACVR2B/Fc treatment also caused moderate hepatomegaly

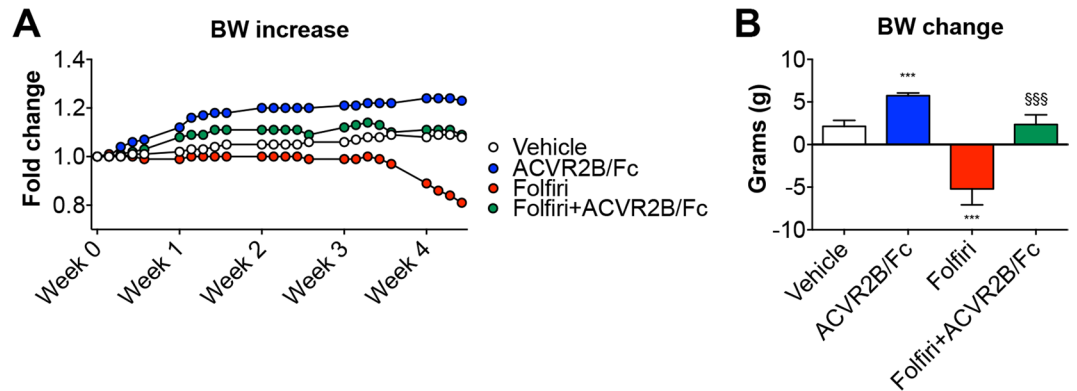


Figure 2. ACVR2B/Fc prevents chemotherapy-induced body weight loss. Body weight curves (A) and body weight change (*i.e.* body weight at time of sacrifice vs. initial body weight) (B) in mice exposed to Folfiri and ACVR2B/Fc for up to 5 weeks ($n = 6-7$). Data expressed as means \pm SD. Significance of the differences: *** $p < 0.001$ vs. Vehicle; \$\$\$ $p < 0.001$ vs. Folfiri.

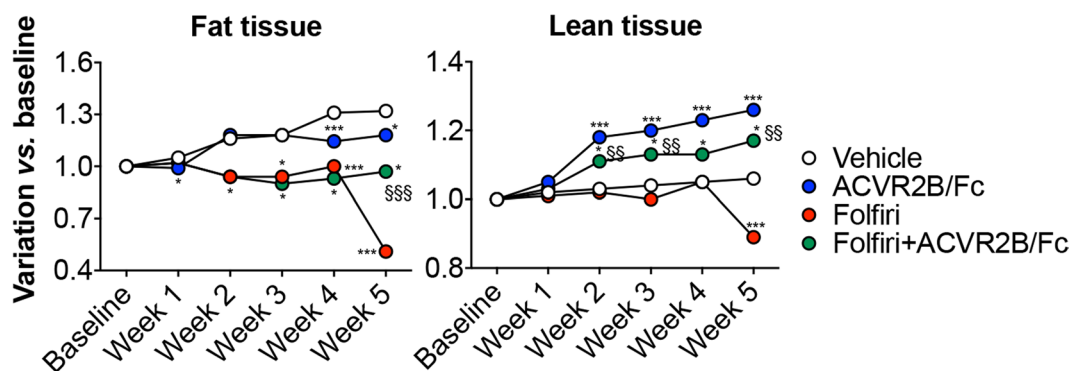


Figure 3. ACVR2B/Fc administration abolishes muscle depletion and partially protects against fat loss in mice treated with Folfiri. Body composition assessment in animals exposed to Folfiri and ACVR2B/Fc ($n = 6-7$) was performed by means of EchoMRI. Data (grams of fat or lean tissue) are expressed as fold change variation vs. baseline (day 0) over 5 weeks. Significance of the differences: * $p < 0.05$, ** $p < 0.01$, *** $p < 0.001$ vs. Vehicle; \$\$\$ $p < 0.01$, \$\$\$ $p < 0.001$ vs. Folfiri.

(+15% vs. Vehicle; $p < 0.01$) and only partially restored the fat tissue in the Folfiri-treated mice (+53% vs. Folfiri; $p < 0.05$). No change in spleen size was recorded in any of the experimental groups (Fig. 5).

ACVR2B/Fc preserves muscle size and muscle strength in animals receiving Folfiri. Similar to Fig. 4, fiber hypertrophy was displayed in the tibialis anterior muscle following treatment with ACVR2B/Fc (+48%; $p < 0.001$ vs. Vehicle), while its administration in combination with chemotherapy presented a complete preservation of fiber size vs. the Folfiri-treated animals (+82%; $p < 0.001$) (Fig. 6A). Weekly ACVR2B/Fc treatment, combined with chemotherapy, not only was able to fully counteract the muscle weakness associated with Folfiri (+38%; $p < 0.001$), but also induced a significant increase in muscle strength respect to the Vehicle-treated animals (+11%; $p < 0.001$) (Fig. 6B).

ACVR2B/Fc prevents Folfiri-induced loss of trabecular bone mass. In order to verify whether the Folfiri-associated effects on skeletal muscle mass were reflected in a similar manner in bone, sections from femurs and vertebrae extracted from animals exposed to Folfiri and ACVR2B/Fc were analyzed by microcomputed tomography. The animals exposed to Folfiri treatment exhibited a severe loss of trabecular bone but not cortical bone in the femur (Fig. 7). This was evidenced by markedly reduced trabecular bone volume fraction (BV/TV; +79%; $p < 0.001$), thickness (Tb.Th; -26%; $p < 0.001$), number (Tb.N; -72%; $p < 0.001$) and connectivity density (Conn.Dn; -39%; $p < 0.01$), as well as increased trabecular separation (Tb.Sp; +91%; $p < 0.001$) vs. Vehicle (Fig. 7A,B). The administration of ACVR2B/Fc alone not only enhanced the trabecular BV/TV (+73%; $p < 0.001$), Tb.Th (+21%; $p < 0.01$) and Tb.N (+44%; $p < 0.001$) vs. the Vehicle-treated mice, but also significantly protected the trabecular bone when combined with Folfiri, as shown by ameliorated BV/TV (+247%; $p < 0.001$), Tb.Th (+42%; $p < 0.001$), Tb.Sp (-36%; $p < 0.001$), Tb.N (+147%; $p < 0.001$) (Fig. 7A,B). Unlike the trabecular bone, the femoral cortical bone was not affected by any of the treatments, as shown by unchanged cortical bone volume fraction (Ct.BV/TV), thickness (Ct.Th) and Porosity (Fig. 7C,D). The vertebral trabecular bone was also affected by Folfiri, as shown by reduced BV/TV (-51%; $p < 0.001$) and Tb.N (-49%; $p < 0.001$),

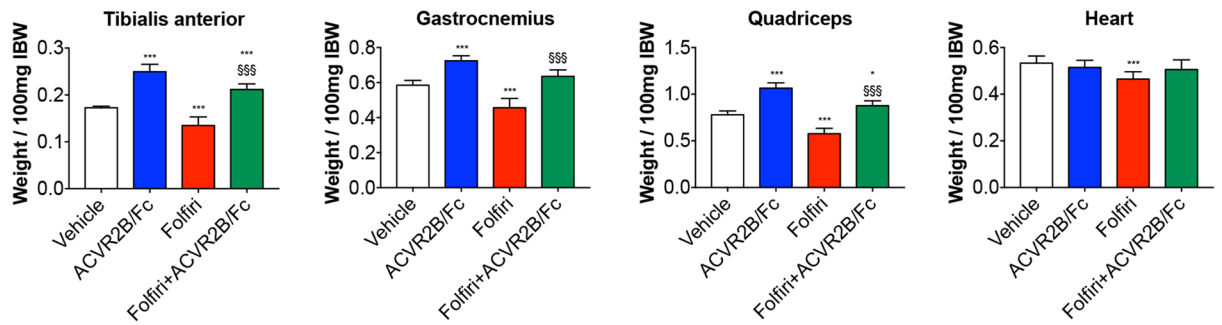


Figure 4. Administration of ACVR2B/Fc prevents muscle atrophy in the Folfiri-treated. Muscle weights in mice treated with Folfiri and ACVR2B/Fc for up to 5 weeks ($n=6-7$). Weights were normalized to the Initial Body Weight (IBW) and expressed as weight/100 mg IBW. Data expressed as means \pm SD. GSN: gastrocnemius. Significance of the differences: * $p < 0.05$, *** $p < 0.001$ vs. Vehicle; \$\$\$ $p < 0.001$ vs. Folfiri.

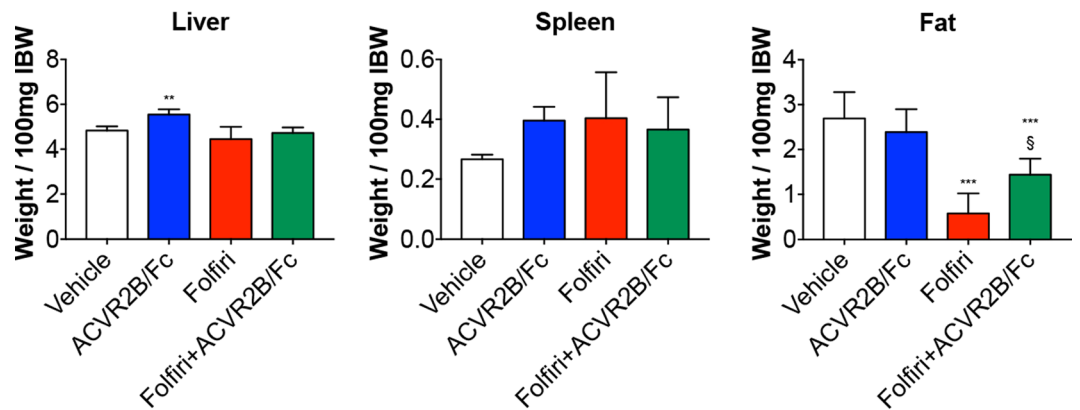


Figure 5. Folfiri-induced adipose tissue depletion is partially prevented by ACVR2B/Fc treatment. Liver, spleen and fat weights in mice treated with Folfiri and ACVR2B/Fc for up to 5 weeks ($n=6-7$). Weights were normalized to the Initial Body Weight (IBW) and expressed as weight/100 mg IBW. Data expressed as means \pm SD. Significance of the differences: ** $p < 0.01$, *** $p < 0.001$ vs. Vehicle; \$ $p < 0.05$ vs. Folfiri.

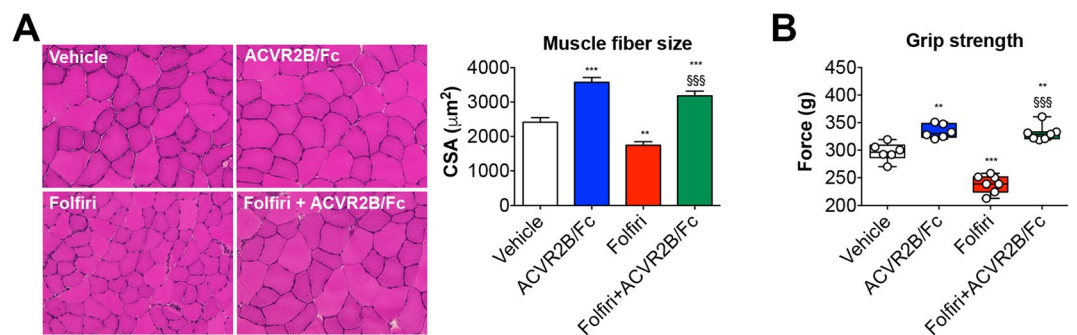


Figure 6. ACVR2B/Fc prevents the Folfiri-associated loss of muscle fiber size and muscle strength. Muscle morphology (H&E staining) and quantification of the cross-sectional area (CSA) in the tibialis anterior muscle of mice exposed to chemotherapy or ACVR2B/Fc. Scale bar: 100 μm . Magnification: 20X (A). Whole body grip strength in animals administered chemotherapy or ACVR2B/Fc for up to 5 weeks, reported as peak force, was measured by taking advantage of a grip strength meter and expressed as the average of the three top pulls from each animal ($n=6-7$) (B). Data expressed as means \pm SD. Significance of the differences: ** $p < 0.01$, *** $p < 0.001$ vs. Vehicle; \$\$\$ $p < 0.001$ vs. Folfiri.

and by increased Tb.Sp (+44%; $p < 0.001$) with respect to the Vehicle-treated mice (Fig. 8A,B). The ACVR2B/Fc administration was able to counteract the Folfiri-associated effects in trabecular bone in both femur and vertebrae, thereby improving BV/TV (+112%; $p < 0.001$), Tb.Th (+17%; $p < 0.05$), Tb.Sp (-28%; $p < 0.001$), Tb.N (+82%; $p < 0.001$) (Fig. 8A,B).

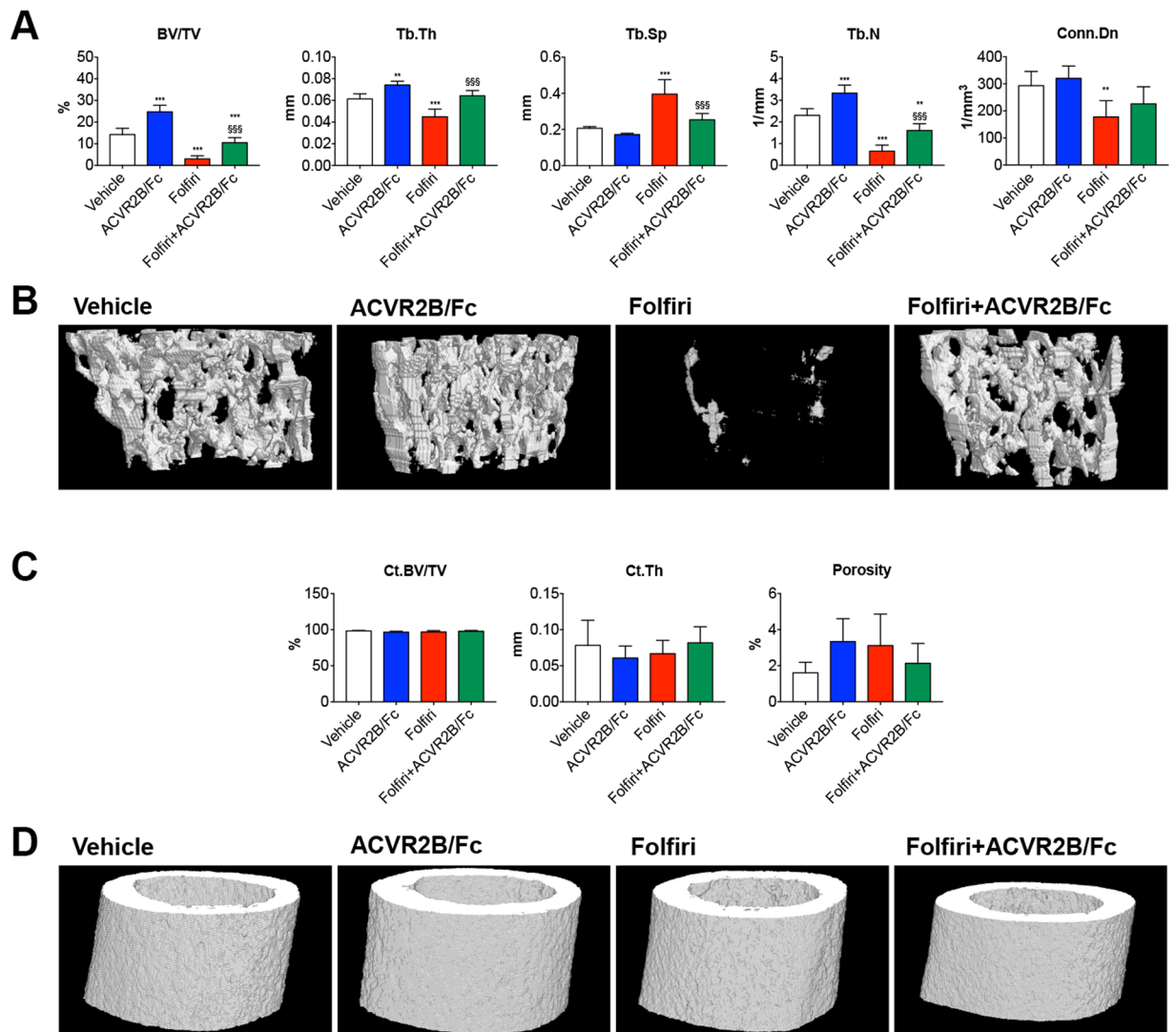


Figure 7. Folfiri severely affects the trabecular bone mass, but not the cortical bone, in the mouse femurs, and ACVR2B/Fc completely abolishes its effects. Quantification of bone volume fraction (BV/TV), trabecular thickness (Tb.Th), trabecular separation (Tb.Sp), trabecular number (Tb.N) and trabecular connectivity density (Conn.Dn) in the femur of mice treated with Folfiri and ACVR2B/Fc ($n = 6-7$) (A). Representative 3D rendering of μ CT scan images of femur sections (B). Quantification of cortical bone volume fraction (Ct. BV/TV), cortical thickness (Ct.Th) and overall porosity in the femur of mice exposed to Folfiri and ACVR2B/Fc ($n = 6-7$) (C). 3D rendering of μ CT scan images of cortical femur sections (D). Data are expressed as means \pm SD. Significance of the differences: * $p < 0.05$, ** $p < 0.01$, *** $p < 0.001$ vs. Vehicle; **** $p < 0.001$ vs. Folfiri.

ACVR2B/Fc reduces IL-6 and activin A in combination with chemotherapy. In order to better understand the effects associated with the administration of ACVR2B/Fc to healthy animals and mice treated with Folfiri, we assessed the circulating levels of IL-6 and activin A, previously reported to play a major role in promoting cachexia and in the regulation of muscle and bone mass^{17,39}. In our animal model, the administration of Folfiri for up to 5 weeks resulted into markedly elevated IL-6 (~36-fold increase vs. Vehicle; $p < 0.001$), which was completely prevented in combination with ACVR2B/Fc ($p < 0.001$ vs. Folfiri) (Fig. 9). On the other hand, despite being more elevated (+93%) following Folfiri treatment, activin A was not statistically different compared to the vehicle-treated animals. Interestingly, the combined administration of ACVR2B/Fc resulted into reduced activin A with respect to the animals receiving Folfiri (-63%; $p < 0.05$) or the vehicle (-30%; $p < 0.05$) (Fig. 9).

Discussion

Cancer development often contributes to the loss of muscle mass and muscle strength, compromising the overall quality of life by decreasing both productivity and physical functioning⁴⁰⁻⁴⁴. Similarly, despite the recent development of novel and more effective treatment strategies capable of significantly improving life expectancy,

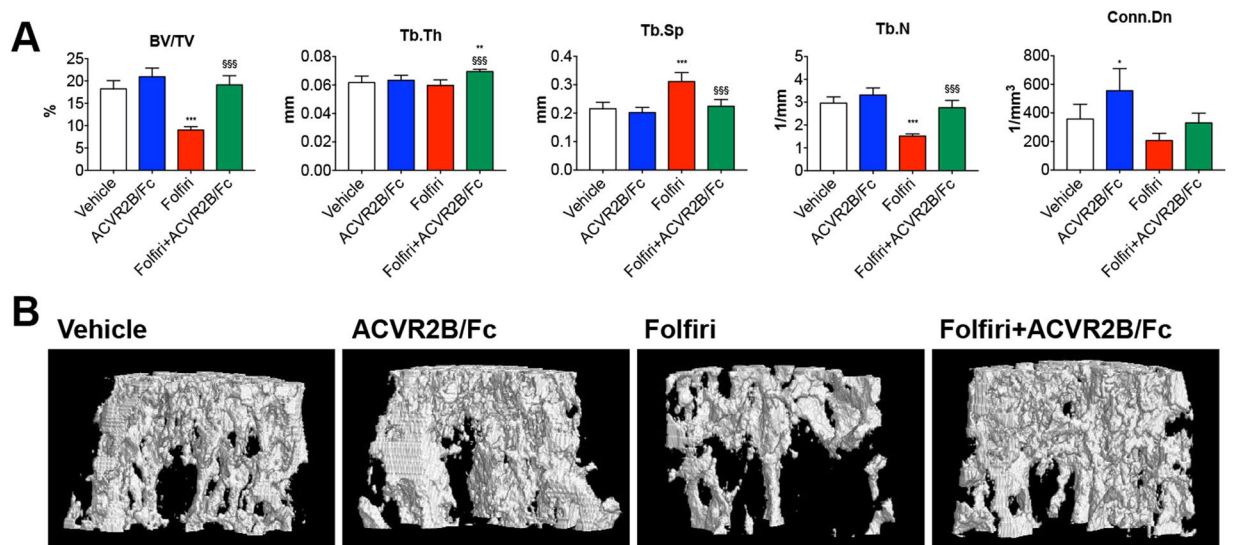


Figure 8. ACVR2B/Fc prevents the Folfiri-mediated effects on vertebral bone tissue. Quantification of bone volume fraction (BV/TV), trabecular thickness (Tb.Th), trabecular separation (Tb.Sp), trabecular number (Tb.N) and trabecular connectivity density (Conn.Dn) in the vertebrae of mice treated with Folfiri and ACVR2B/Fc ($n = 6-7$) (A). Representative 3D rendering of μ CT scan images of vertebral sections (B). Data are expressed as means \pm SD. Significance of the differences: * $p < 0.05$, *** $p < 0.001$ vs. Vehicle; \$\$\$ $p < 0.001$ vs. Folfiri.

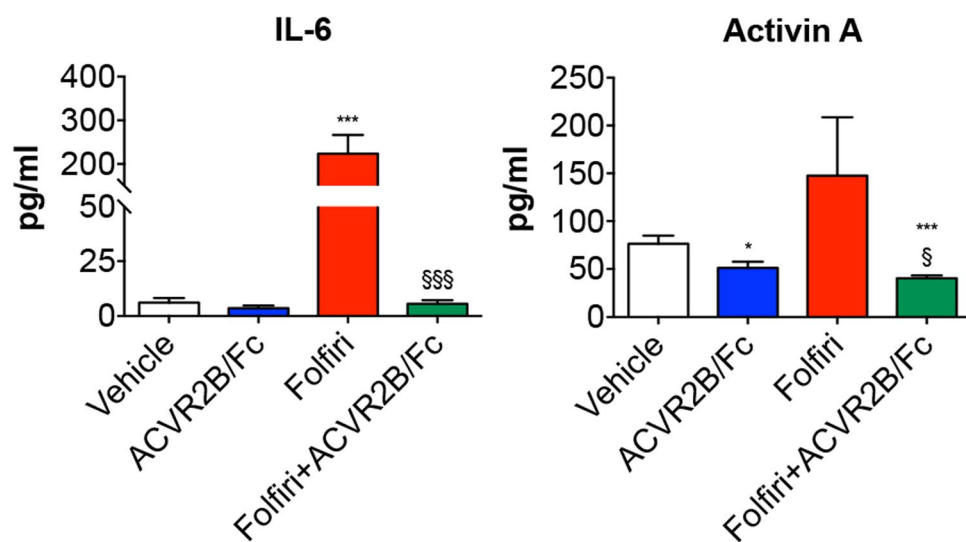


Figure 9. ACVR2B/Fc treatment potently reduces IL-6 and Activin A circulating levels in combination with Folfiri. Quantification of IL-6 and Activin A levels in the plasma from mice exposed to Folfiri, alone or in combination with ACVR2B/Fc ($n = 6-7$). Data, expressed as means \pm SD, are reported in pg/ml. Significance of the differences: *** $p < 0.001$ vs. Vehicle; \$ $p < 0.05$, \$\$\$ $p < 0.001$ vs. Folfiri.

the administration of anti-cancer therapies is known to adversely affect patients' quality of life by producing mild-to-severe side effects. Nausea, diarrhea, anorexia and increased fatigue are the most relevant⁴⁵⁻⁴⁷.

We and others have reported that anti-cancer therapies cause a decline of muscle size and function (*i.e.* cachexia) in both animal models and cancer patients^{17,47-50}. Notably, the chemotherapy-associated muscle functional deficits have been shown to positively correlate with both enhanced mortality^{2,51} and aggressiveness of chemotherapy^{52,53}. Further, these complications have been reported to cause difficulty for patients to adhere to or complete treatment regimens, for delays in treatment, to cause dose limitation, and for discontinuation of therapy in cancer patients^{54,55}. No remedies have been identified to relieve such conditions thus far, and the chemotherapy-associated muscle defects have been shown to persist for months to years following remission^{17,56-62}.

In a similar manner, significant loss of bone mass was described in patients undergoing adjuvant chemotherapy for various gynecologic cancers^{63,64} and radiotherapy for abdominal tumors⁶⁵. A variety of hormonal and non-hormonal compounds, frequently used in patients affected with breast and prostate cancer, was shown to promote bone resorption and bone turnover. This contributed to the development of bone loss and to the exacerbation of the overall mortality⁷. Therefore, the occurrence of bone fractures in patients with cancer or undergoing chemo-radiotherapy represents a problem of significant concern and deserves major attention.

Over the past 50 years, fluoropyrimidines, such as 5-fluorouracil (5-FU), have remained one of the most commonly used antimetabolite drugs. They have been prescribed for the therapy of metastatic colorectal cancers, resulting in significant increases in survival rates, particularly in combination with leucovorin⁶⁶ and irinotecan, a topoisomerase I inhibitor⁶⁷. This treatment regimen, known as Folfiri, is routinely used as a first-line chemotherapy regimen for the treatment of metastatic colorectal cancer alone, and can also be used in combination with other anti-cancer compounds, such as bevacizumab, aflibercept, cetuximab or panitumumab, to improve efficacy and response rates^{68,69}.

In the present study we investigated the muscle and bone toxicities associated with the administration of Folfiri. This systemic chemotherapy regimen can have a major impact on patients' quality of life and is often responsible for severe side effects, including myelotoxicity, gastrointestinal toxicity, enhanced morbidity and occasional mortality⁷⁰. In line with our previous findings¹⁷, we report that prolonged *in vivo* Folfiri treatment accounts for severe effects on skeletal and to a lesser extent, cardiac muscles, in both male and female mice. Progressive loss of myofiber size and muscle strength occurs in animals exposed to this treatment for up to 5 weeks. Folfiri is also associated with a marked loss of adipose tissue, thereby contributing to the establishment of a general cachectic phenotype^{17,39}. Interestingly, the effects described in the females were less pronounced, suggesting that gender-specific effects may play a role in determining drug toxicity. This is also in line with previous reports showing that females are likely more resistant to high-dose chemotherapy and have increased likelihood of receiving second-line anti-cancer therapies for the treatment of lung cancer⁷¹⁻⁷³.

We also showed for the first time that chronic administration of Folfiri also associates with unexpected and severe trabecular bone loss in normal animals. Ours is not the first report to show that anti-cancer drugs may affect bone strength and quality. Indeed, Fonseca *et al.* previously reported that anti-cancer drugs, such as doxorubicin, routinely used in pediatric cancer treatment, not only promote muscle wasting³⁵, but also negatively affects the overall bone morphology, as well as the femur mechanical properties in rats⁷⁴. This is of particular importance, especially considering that patients affected with metastatic colorectal cancer usually undergo multiple rounds of chemotherapy treatment, thereby having far more chances to develop such toxicity. In addition we found that the cortical bone, however, did not seem to be significantly affected, at least within this time frame. This apparent discrepancy could be interpreted by the fact that the cortical bone, which accounts for 80% of the adult human skeleton, is typically less metabolically active than the trabecular bone⁷⁵, and therefore likely less susceptible of the anti-proliferative and cytotoxic effects associated with the administration of chemotherapy. These effects may also be explained by the fact that 5-FU, one of the main components of the Folfiri regimen, was shown to cause marked bone loss in rats after only five consecutive days of treatment, possibly by inducing inflammation, suppressing osteoblast activity and enhancing osteoclast recruitment, therefore promoting an unbalance in bone remodeling⁷⁶. Recent findings from Fen *et al.* showed that six cycles of 5-FU combined with cyclophosphamide and epirubicin, one of the preferred chemotherapy regimens for the treatment of breast cancer, were able to promote severe loss of trabecular bone, reduction of bone marrow cells and marrow adiposity in experimental animals⁷⁷.

The investigation of muscle/bone crosstalk has failed to identify new targets for the treatment of chemotherapy-associated muscle wasting and osteoporosis. Unfortunately, only a few therapies, characterized by high cost and occasional long-term toxicities, are available to date. They include anti-resorptive drugs, such as the bisphosphonates, which are routinely used for the treatment and prevention of osteoporosis and bone fractures in cancer patients^{78,79}. Despite this, several side effects, such as acute-phase reactions, nephrotoxicity, hypocalcemia and osteonecrosis of the jaw, have been reported²⁷. On the other hand, the PTH peptides represent the only approved anabolic therapy currently in use to promote bone formation relative to bone resorption⁸⁰, a process that primarily affects the trabecular bone tissue, whereas the effects on the cortical bone are somewhat modest and may depend on the degree of mechanical loading⁸¹. Safety and tolerability of these compounds, especially after prolonged administration, are still under debate, and their use in cancer patients is being evaluated. Indeed, the 2-year chronic administration of teriparatide, or rhPTH(1-34), a synthetic agonist of human PTH currently under investigation for the treatment of postmenopausal osteoporosis, was shown to potentially impact carcinogenicity by causing the formation of osteosarcomas in F344 rats, although the same finding has not been reported in the clinical setting thus far^{82,83}. Moreover, despite their beneficial effects on bone mass, PTH and PTH-related protein (PTHrP) have been described to affect muscle size through the common PTH receptor (PTHrR)²⁸⁻³⁰, therefore raising concerns that the administration of PTH peptide in patients with cancer or treated with chemotherapy, that are already at risk of significant muscle loss, may instead exacerbate their cachectic condition. Overall, it is known that muscle targeted pro-anabolic strategies can improve survival and quality of life in cancer^{31,32}, as well as reduce the toxicity of anticancer drugs^{17,36}. Conversely, it is not completely clear whether drugs aimed at primarily preserving bone tissue also play a role in improving the overall outcomes in the presence of a tumor. As a matter of fact, no conclusive effects of bisphosphonate administration on delayed cancer recurrence and improved survival rates have been reported so far⁸⁴. Similarly, it is also uncertain if bisphosphonate treatment benefits muscle size and function.

In the present study we showed that inhibition of the signaling of the activin type 2B receptor represents a potent therapeutic strategy to prevent both muscle and bone loss following chemotherapy treatment. Indeed, in our study ACVR2B/Fc, a synthetic fusion peptide inhibitor of the activin receptor type 2B, was able to fully restore muscle size and function in cachectic Folfiri-treated mice. This concurs with our previous observations

conducted *in vitro* using a model of chemotherapy-associated myofiber atrophy¹⁷. For instance, other reports suggest that the blockade of this signaling pathway mitigates the loss of muscle mass and strength in the presence of muscle atrophy due to cancer^{31,32} or its treatments^{35,36}, AIDS⁸⁵, muscular dystrophy^{38,86} or disuse⁷⁸. ACVR2B/Fc also completely abolished the loss of bone tissue by fully preserving the trabecular bone in the animals exposed to Folfiri, as shown by the μ CT analysis. Our results are consistent with previous observations reporting beneficial effects of ACVR2B/Fc treatment in mice affected with type III osteogenesis imperfecta³⁷ or muscular dystrophy³⁸, further showing substantial preservation of bone mass and mechanical properties. Similar to the previously published findings⁷⁹, ACVR2B/Fc displayed bone anabolic properties, as suggested by increased trabecular bone volume fraction, thickness and number in the femurs of normal mice. Conversely, we did not observe any increase in vertebral bone parameters, with the exception of Conn.Dn, in disagreement with Bialek *et al.*⁷⁹ Of note, no effect of ACVR2B/Fc treatment was observed in cortical bone in our model, in line with prior evidence⁷⁹.

Overall, the abnormal activation of the signaling pathway downstream of the activin receptors is known to play a role in the regulation of both muscle and bone crosstalk, although whether the activin signaling plays a more relevant role in promoting bone abnormalities by specifically affecting either the trabecular or the cortical bone remains to be elucidated. Cancer-associated changes in the circulating levels of activin family ligands, including activin A, activin B, myostatin and GDF-11, are known to exert effects on muscle and bone homeostasis, thus contributing to the development of overt cachexia^{87–89}. Similarly, Waning *et al.* suggested that the release of TGF β due to the presence of breast cancer-associated metastatic bone lesions is responsible for muscle depletion and weakness⁹⁰. Further, activin A, also known as a negative regulator of muscle mass and an independent prognosis factor of survival in cancer patients^{88,91,92}, was described elevated in the bone matrix and was reported to play a role in the regulation of osteoclast induction and bone remodeling^{93–96}. Conversely, its inhibition by means of a ligand trap soluble receptor was shown to induce bone formation and bone strength in normal and diabetic mice, as well as in ovariectomized mice affected with bone loss^{97,98}. Additionally, pro-inflammatory cytokines, such as IL-1, IL-6 and TNF, known for their pro-catabolic and anti-anabolic effects in muscle tissue and for their relevant role in the pathogenesis of cachexia^{99–102}, have also been shown to interact with activin A by exacerbating its detrimental effects in skeletal muscle^{103,104}. In the present study we showed that IL-6 was elevated following chemotherapy treatment, and that such effect was potently counteracted by ACVR2B/Fc administration. This is in contrast with the data reported by Zhou *et al.*, showing no effect of ACVR2B/Fc treatment on IL-6 levels in the presence of the C26 tumor³². On the other hand, circulating activin A levels did not seem to be affected by the Folfiri treatment, despite a trend towards higher concentrations that was not statistically significant, also in line with our initial observations reported in muscle tissue¹⁷. However, we should mention that in our work activin A was only assessed at time of sacrifice (*i.e.* three days after the last Folfiri injection; Fig. 1), therefore we cannot exclude that higher levels of the same factor may be detected at earlier time points or shortly after chemotherapy treatment.

Collectively, the present study shows that depletion of bone tissue occurs concurrently with severe loss of muscle mass and function in normal animals exposed to Folfiri. It also validates the blockade of the ACVR2B-dependent pathway as a potential new strategy aimed at benefitting cachectic cancer patients undergoing chemotherapy. Based on our and other's previous observations^{17,35,77,105}, the animal model used in this study represents an effective tool to study the musculoskeletal effects of anti-cancer drugs *in vivo*, a condition that must be fulfilled in order to generate meaningful animal results for human translation. Regardless, we are aware that this may also represent a limitation of our study, due to the fact that in the clinical setting only subjects affected with cancer are normally treated with chemotherapy, therefore possibly preventing us from identifying those interactions between tumor- and chemotherapy-driven mediators that may be ultimately responsible for the muscle and bone phenotypic alterations.

Furthermore, our data further support the concept that significant communication occurs in normal physiology between two closely related organs, such as muscle and bone¹⁰⁶. Indeed, muscle tissue generally behaves as an endocrine organ for 'myokines' (*e.g.*, IL-6, myostatin, IGF-1) playing a role in bone metabolism and function^{106–109}. Conversely, bone acts as a storehouse of 'osteokines' (*e.g.*, activin A, TGF β , osteocalcin) released in physiologic and pathologic conditions, affecting the functionality of several organs, including skeletal muscle^{90,110–116}. Despite all this, it is not yet known which tissue primarily influences the metabolism and function of the other, and whether the bone derangements precede the muscle effects, or vice versa. Additional efforts will be required to establish new strategies aimed at detecting early cancer-associated musculoskeletal deficits and at counteracting the simultaneous loss of muscle and bone mass following cancer treatments, especially taking into consideration that interventions primarily designed to promote muscle growth may also exert beneficial effects on bone mass, as well as bone-targeted strategies may additionally benefit skeletal muscle and its function.

Methods

Animals. All animal studies were approved by the Institutional Animal Care and Use Committee at Indiana University School of Medicine and were in compliance with the National Institutes of Health Guidelines for Use and care of Laboratory Animals and with the 1964 Declaration of Helsinki and its later amendments. For all the experiments described, animals were identified with a code and the investigators were blinded during allocation, animal handling, and endpoint measurements. Animals (up to 5 per cage) were housed in a pathogen-free facility at IU LARC. Male ($n = 6–7$) and female ($n = 5$) immunocompetent CD2F1 mice (Envigo, Indianapolis, IN) were used. However, after an initial characterization of the muscle-specific effects associated with Folfiri treatment alone, only the male mice were examined to investigate the beneficial effects of ACVR2B/Fc administration, in continuation with our initial study aimed at determining the effects of commonly-used chemotherapeutics on muscle mass and function¹⁷. More specifically, the male mice were randomized into four groups, namely Vehicle ($n = 6$), ACVR2B/Fc ($n = 6$), Folfiri ($n = 7$) and Folfiri + ACVR2B/Fc ($n = 7$). The Folfiri-treated animals received Folfiri (50 mg/kg 5-Fluorouracil, 90 mg/kg Leucovorin, 24 mg/kg Irinotecan) intraperitoneally (*i.p.*) twice weekly

for up to 5 consecutive weeks¹⁷. The ACVR2B/Fc groups were administered the synthetic peptide once weekly (10 mg/kg in sterile PBS; i.p.). The Vehicle-treated animals received equal volumes of solvents only. The animals were weighed daily. At sacrifice, several tissues, including skeletal muscles, were collected, weighed, frozen in liquid nitrogen and stored at -80°C for further studies. The tibialis anterior muscles were rapidly excised, mounted in OCT and frozen in N_2 -cooled isopentane for histology, as previously described¹⁷. The mouse carcasses were fixed for 2 days in 10% neutral buffered formalin, and then transferred into 70% ethanol for storage of bone and other tissues. All chemotherapy drugs were purchased from Sigma Aldrich (St. Louis, MO). ACVR2B/Fc was purified from CHO-ACVR2B/Fc conditioned medium¹¹⁸.

Grip strength. The evaluation of the whole body strength in mice was assessed as described in¹¹⁹. Briefly, the absolute grip strength (expressed in grams) was recorded by means of grip strength meter (Columbus Instruments, Columbus, OH). Overall, 5 measurements were completed and only the top three measurements were included in the analysis. In order to avoid habituation, the animals were tested for grip strength no more than once weekly.

Body composition assessment. Body composition, e.g. the quantification of lean (muscle) and fat (adipose) mass, was measured once weekly over the entire duration of the experiment in un-anesthetized but physically restrained mice by means of an Echo Medical systems' EchoMRI-100 (EchoMRI, Houston, USA), as shown in¹⁷. This is a moderately stressful analysis, therefore the animals were assessed no more than once weekly. Data were expressed as variations over the baseline values.

Measurement of muscle cross-sectional area (CSA). Ten μm -thick cryosections of tibialis anterior muscles taken at the mid-belly were processed for Hematoxylin & Eosin staining. All samples were observed under an Axio Observer.Z1 motorized microscope (Zeiss, Oberchoken, Germany) and images were recorded for morphometric examination. For determination of the cross-sectional area (CSA), muscle fibers ($n = 300\text{--}500$ per sample) were measured by tracing the perimeter of each individual fiber using a Cintiq pen tablet input device (Wacom, Vancouver, WA, USA) and Image J 1.43 software¹²⁰.

Micro computed tomography (μCT) analysis of femurs and vertebrae bone morphology. MicroCT (μCT) scanning was performed to measure morphological indices of metaphyseal regions of femurs and vertebrae, as described in¹²¹. After euthanasia, the mouse carcasses were fixed for 2 days in 10% neutral buffered formalin, transferred into 70% ethanol, the right femurs and the fifth lumbar vertebrae dissected, and prepared for μCT scanning on a high-throughput μCT specimen scanner. Bone samples were rotated around their long axes and images were acquired using a Bruker Skyscan 1176 (Bruker, Kontich, Belgium) with the following parameters: pixel size = $9\ \mu\text{m}^3$; peak tube potential = 50 kV; X-ray intensity = 500 μA ; 0.9° rotation step. Raw images were reconstructed using SkyScan reconstruction software (NRecon; Bruker, Kontich, Belgium) to 3-dimensional cross-sectional image data sets using a 3-dimensional cone beam algorithm. Structural indices were calculated on reconstructed images using the Skyscan CT Analyzer software (CTAn; Bruker, Kontich, Belgium). Cortical and trabecular bone were separated using a custom processing algorithm in CTAn, based on the different thicknesses of the structures. Cortical bone was analyzed by threshold 160–255 in the femoral mid-shaft. Cortical bone parameters included bone volume fraction (Ct.BV/TV), thickness (Ct.Th), and porosity. Trabecular bone was analyzed between 2.0 mm to 3.0 mm under the femoral distal growth plate and 1 mm equally between the distal and proximal growth plates in the fifth lumbar vertebra using a threshold of 80–255. Trabecular parameters included bone volume fraction (Tb.BV/TV), number (Tb.N), thickness (Tb.Th), separation (Tb.Sp), and connectivity (Conn.Dn).

Quantification of circulating IL-6 and activin A. The circulating levels of Activin A (#DAC00B) and IL-6 (#M6000B) were measured in mouse poor-platelet plasma by using specific ELISA kits (Bio-Techne Corporation, Minneapolis, MN) and following the manufacturer's protocol.

Statistical analysis. Results are presented as means \pm SD. Significance of the differences was determined by analysis of variance (ANOVA) followed by Tukey's post-test. Differences were considered significant when $p < 0.05$.

References

1. Siegel, R. L., Miller, K. D. & Jemal, A. Cancer Statistics, 2017. *CA: a cancer journal for clinicians* **67**, 7–30, <https://doi.org/10.3322/caac.21387> (2017).
2. Fearon, K. *et al.* Definition and classification of cancer cachexia: an international consensus. *The lancet oncology* **12**, 489–495, [https://doi.org/10.1016/S1470-2045\(10\)70218-7](https://doi.org/10.1016/S1470-2045(10)70218-7) (2011).
3. Costelli, P. & Baccino, F. M. Mechanisms of skeletal muscle depletion in wasting syndromes: role of ATP-ubiquitin-dependent proteolysis. *Current opinion in clinical nutrition and metabolic care* **6**, 407–412, <https://doi.org/10.1097/01.mco.0000078984.18774.02> (2003).
4. Tisdale, M. J. Mechanisms of cancer cachexia. *Physiological reviews* **89**, 381–410, <https://doi.org/10.1152/physrev.00016.2008> (2009).
5. Fearon, K. C., Glass, D. J. & Guttridge, D. C. Cancer cachexia: mediators, signaling, and metabolic pathways. *Cell metabolism* **16**, 153–166, <https://doi.org/10.1016/j.cmet.2012.06.011> (2012).
6. Haehling, S. V. & Anker, S. D. Cachexia as a major underestimated and unmet medical need: facts and numbers. *Journal of Cachexia, Sarcopenia and Muscle* **1**, 1–5 (2010).
7. Coleman, R. E. Clinical features of metastatic bone disease and risk of skeletal morbidity. *Clinical cancer research: an official journal of the American Association for Cancer Research* **12**, 6243s–6249s, <https://doi.org/10.1158/1078-0432.CCR-06-0931> (2006).
8. DeSantis, C. E. *et al.* Cancer treatment and survivorship statistics, 2014. *CA: a cancer journal for clinicians* **64**, 252–271, <https://doi.org/10.3322/caac.21235> (2014).

9. Bonetto, A. *et al.* Differential Bone Loss in Mouse Models of Colon Cancer Cachexia. *Front Physiol* **7**, 679, <https://doi.org/10.3389/fphys.2016.00679> (2017).
10. Pedroso, F. E. *et al.* Inflammation, organomegaly, and muscle wasting despite hyperphagia in a mouse model of burn cachexia. *Journal of cachexia, sarcopenia and muscle* **3**, 199–211, <https://doi.org/10.1007/s13539-012-0062-x> (2012).
11. Silbermann, R. & Roodman, G. D. Myeloma bone disease: Pathophysiology and management. *J Bone Oncol* **2**, 59–69, <https://doi.org/10.1016/j.jbo.2013.04.001> (2013).
12. Choi, E. *et al.* Concurrent muscle and bone deterioration in a murine model of cancer cachexia. *Physiol Rep* **1**, e00144, <https://doi.org/10.1002/phy2.144> (2013).
13. Greco, S. H. *et al.* TGF-beta Blockade Reduces Mortality and Metabolic Changes in a Validated Murine Model of Pancreatic Cancer Cachexia. *PLoS one* **10**, e0132786, <https://doi.org/10.1371/journal.pone.0132786> (2015).
14. Curt, G. A. *et al.* Impact of cancer-related fatigue on the lives of patients: new findings from the Fatigue Coalition. *The oncologist* **5**, 353–360 (2000).
15. Glaus, A. Assessment of fatigue in cancer and non-cancer patients and in healthy individuals. *Supportive care in cancer: official journal of the Multinational Association of Supportive Care in Cancer* **1**, 305–315 (1993).
16. Guise, T. A. Bone loss and fracture risk associated with cancer therapy. *The oncologist* **11**, 1121–1131, <https://doi.org/10.1634/theoncologist.11-10-1121> (2006).
17. Barreto, R. *et al.* Chemotherapy-related cachexia is associated with mitochondrial depletion and the activation of ERK1/2 and p38 MAPKs. *Oncotarget* **7**, 43442–43460, <https://doi.org/10.18632/oncotarget.9779> (2016).
18. Shandala, T. *et al.* The role of osteocyte apoptosis in cancer chemotherapy-induced bone loss. *Journal of cellular physiology* **227**, 2889–2897, <https://doi.org/10.1002/jcp.23034> (2012).
19. Williams, H. J. & Davies, A. M. The effect of X-rays on bone: a pictorial review. *Eur Radiol* **16**, 619–633, <https://doi.org/10.1007/s00330-005-0010-7> (2006).
20. Bines, J., Oleske, D. M. & Cobleigh, M. A. Ovarian function in premenopausal women treated with adjuvant chemotherapy for breast cancer. *Journal of clinical oncology: official journal of the American Society of Clinical Oncology* **14**, 1718–1729, <https://doi.org/10.1200/JCO.1996.14.5.1718> (1996).
21. Hadji, P. *et al.* Cancer treatment-induced bone loss in premenopausal women: a need for therapeutic intervention? *Cancer Treat Rev* **38**, 798–806, <https://doi.org/10.1016/j.ctrv.2012.02.008> (2012).
22. Cameron, D. A., Douglas, S., Brown, J. E. & Anderson, R. A. Bone mineral density loss during adjuvant chemotherapy in premenopausal women with early breast cancer: is it dependent on oestrogen deficiency? *Breast Cancer Res Treat* **123**, 805–814, <https://doi.org/10.1007/s10549-010-0899-7> (2010).
23. Nurmio, M. *et al.* Receptor tyrosine kinase inhibition causes simultaneous bone loss and excess bone formation within growing bone in rats. *Toxicol Appl Pharmacol* **254**, 267–279, <https://doi.org/10.1016/j.taap.2011.04.019> (2011).
24. Tannock, I. F. *et al.* Docetaxel plus prednisone or mitoxantrone plus prednisone for advanced prostate cancer. *The New England journal of medicine* **351**, 1502–1512, <https://doi.org/10.1056/NEJMoa040720> (2004).
25. de Bono, J. S. *et al.* Prednisone plus cabazitaxel or mitoxantrone for metastatic castration-resistant prostate cancer progressing after docetaxel treatment: a randomised open-label trial. *Lancet* **376**, 1147–1154, [https://doi.org/10.1016/S0140-6736\(10\)61389-X](https://doi.org/10.1016/S0140-6736(10)61389-X) (2010).
26. Muscaritoli, M. *et al.* Consensus definition of sarcopenia, cachexia and pre-cachexia: joint document elaborated by Special Interest Groups (SIG) “cachexia-anorexia in chronic wasting diseases” and “nutrition in geriatrics”. *Clinical nutrition* **29**, 154–159, <https://doi.org/10.1016/j.clnu.2009.12.004> (2010).
27. Biskup, E., Cai, F. & Vetter, M. Bone targeted therapies in advanced breast cancer. *Swiss Med Wkly* **100**, w14440, doi:smw.2017.14440 (2017).
28. Kir, S. *et al.* PTH/PTHrP Receptor Mediates Cachexia in Models of Kidney Failure and Cancer. *Cell metabolism* **23**, 315–323, <https://doi.org/10.1016/j.cmet.2015.11.003> (2016).
29. Kir, S. *et al.* Tumour-derived PTH-related protein triggers adipose tissue browning and cancer cachexia. *Nature* **513**, 100–104, <https://doi.org/10.1038/nature13528> (2014).
30. Thomas, S. S. & Mitch, W. E. Parathyroid hormone stimulates adipose tissue browning: a pathway to muscle wasting. *Current opinion in clinical nutrition and metabolic care* **20**, 153–157, <https://doi.org/10.1097/MCO.0000000000000357> (2017).
31. Benny Klimek, M. E. *et al.* Acute inhibition of myostatin-family proteins preserves skeletal muscle in mouse models of cancer cachexia. *Biochemical and biophysical research communications* **391**, 1548–1554, <https://doi.org/10.1016/j.bbrc.2009.12.123> (2010).
32. Zhou, X. *et al.* Reversal of cancer cachexia and muscle wasting by ActRIIB antagonism leads to prolonged survival. *Cell* **142**, 531–543, <https://doi.org/10.1016/j.cell.2010.07.011> (2010).
33. Morine, K. J. *et al.* Activin IIB receptor blockade attenuates dystrophic pathology in a mouse model of Duchenne muscular dystrophy. *Muscle Nerve* **42**, 722–730, <https://doi.org/10.1002/mus.21743> (2010).
34. Lee, S. J. *et al.* Regulation of muscle growth by multiple ligands signaling through activin type II receptors. *Proceedings of the National Academy of Sciences of the United States of America* **102**, 18117–18122, <https://doi.org/10.1073/pnas.0505996102> (2005).
35. Nissinen, T. A. *et al.* Systemic blockade of ACVR2B ligands prevents chemotherapy-induced muscle wasting by restoring muscle protein synthesis without affecting oxidative capacity or atrogenes. *Sci Rep* **6**, 32695, <https://doi.org/10.1038/srep32695> (2016).
36. Hatakeyama, S. *et al.* ActRII blockade protects mice from cancer cachexia and prolongs survival in the presence of anti-cancer treatments. *Skelet Muscle* **6**, 26, <https://doi.org/10.1186/s13395-016-0098-2> (2016).
37. DiGirolamo, D. J., Singhal, V., Chang, X., Lee, S. J. & Germain-Lee, E. L. Administration of soluble activin receptor 2B increases bone and muscle mass in a mouse model of osteogenesis imperfecta. *Bone Res* **3**, 14042, <https://doi.org/10.1038/boneres.2014.42> (2015).
38. Puolakkainen, T. *et al.* Treatment with soluble activin type IIB-receptor improves bone mass and strength in a mouse model of Duchenne muscular dystrophy. *BMC Musculoskelet Disord* **18**, 20, <https://doi.org/10.1186/s12891-016-1366-3> (2017).
39. Barreto, R. *et al.* Cancer and chemotherapy contribute to muscle loss by activating common signaling pathways. *Frontiers in Physiology* **7**, 472, <https://doi.org/10.3389/fphys.2016.00472> (2016).
40. Cella, D., Peterman, A., Passik, S., Jacobsen, P. & Breitbart, W. Progress toward guidelines for the management of fatigue. *Oncology (Williston Park)* **12**, 369–377 (1998).
41. Jacobsen, P. B. *et al.* Fatigue in women receiving adjuvant chemotherapy for breast cancer: characteristics, course, and correlates. *J Pain Symptom Manage* **18**, 233–242 (1999).
42. Nail, L. M. Fatigue in patients with cancer. *Oncol Nurs Forum* **29**, 537, <https://doi.org/10.1188/02.ONF.537-546> (2002).
43. Mock, V. *et al.* Fatigue and quality of life outcomes of exercise during cancer treatment. *Cancer Pract* **9**, 119–127 (2001).
44. Montazeri, A. Quality of life data as prognostic indicators of survival in cancer patients: an overview of the literature from 1982 to 2008. *Health Qual Life Outcomes* **7**, 102, <https://doi.org/10.1186/1477-7525-7-102> (2009).
45. D’Oronzo, S., Stucci, S., Tucci, M. & Silvestris, F. Cancer treatment-induced bone loss (CTIBL): pathogenesis and clinical implications. *Cancer Treat Rev* **41**, 798–808, <https://doi.org/10.1016/j.ctrv.2015.09.003> (2015).
46. Montagnani, F., Chiriatti, A., Turrisi, G., Francini, G. & Fiorentini, G. A systematic review of FOLFOXIRI chemotherapy for the first-line treatment of metastatic colorectal cancer: improved efficacy at the cost of increased toxicity. *Colorectal disease: the official journal of the Association of Coloproctology of Great Britain and Ireland* **13**, 846–852, <https://doi.org/10.1111/j.1463-1318.2010.02206.x> (2011).

47. Ahlberg, K., Ekman, T., Gaston-Johansson, F. & Mock, V. Assessment and management of cancer-related fatigue in adults. *Lancet* **362**, 640–650, [https://doi.org/10.1016/S0140-6736\(03\)14186-4](https://doi.org/10.1016/S0140-6736(03)14186-4) (2003).
48. Stasi, R., Abriani, L., Beccaglia, P., Terzoli, E. & Amadori, S. Cancer-related fatigue: evolving concepts in evaluation and treatment. *Cancer* **98**, 1786–1801, <https://doi.org/10.1002/cncr.11742> (2003).
49. Patrick, D. L. *et al.* National Institutes of Health State-of-the-Science Conference Statement: Symptom management in cancer: pain, depression, and fatigue, July 15–17, 2002. *J Natl Cancer Inst Monogr*, 9–16, doi:<https://doi.org/10.1093/jncimonographs/djg014> (2004).
50. NHLBI Workshop summary. Respiratory muscle fatigue. Report of the Respiratory Muscle Fatigue Workshop Group. *Am Rev Respir Dis* **142**, 474–480, doi:<https://doi.org/10.1164/ajrccm/142.2.474> (1990).
51. Evans, W. J. *et al.* Cachexia: a new definition. *Clinical nutrition* **27**, 793–799, <https://doi.org/10.1016/j.clnu.2008.06.013> (2008).
52. Jacobsen, P. B. *et al.* Fatigue after treatment for early stage breast cancer: a controlled comparison. *Cancer* **110**, 1851–1859, <https://doi.org/10.1002/cncr.22993> (2007).
53. Prue, G., Allen, J., Gracey, J., Rankin, J. & Cramp, F. Fatigue in gynecological cancer patients during and after anticancer treatment. *J Pain Symptom Manage* **39**, 197–210, <https://doi.org/10.1016/j.jpainsymman.2009.06.011> (2010).
54. Rosenthal, M. A. & Oratz, R. Phase II clinical trial of recombinant alpha 2b interferon and 13 cis retinoic acid in patients with metastatic melanoma. *Am J Clin Oncol* **21**, 352–354 (1998).
55. Visovsky, C. & Schneider, S. M. Cancer-related fatigue. *Online J Issues Nurs* **8**, 8 (2003).
56. Brown, D. J., McMillan, D. C. & Milroy, R. The correlation between fatigue, physical function, the systemic inflammatory response, and psychological distress in patients with advanced lung cancer. *Cancer* **103**, 377–382, <https://doi.org/10.1002/cncr.20777> (2005).
57. Galvao, D. A. *et al.* Reduced muscle strength and functional performance in men with prostate cancer undergoing androgen suppression: a comprehensive cross-sectional investigation. *Prostate Cancer Prostatic Dis* **12**, 198–203, <https://doi.org/10.1038/pcan.2008.51> (2009).
58. Hayes, S., Battistutta, D. & Newman, B. Objective and subjective upper body function six months following diagnosis of breast cancer. *Breast Cancer Res Treat* **94**, 1–10, <https://doi.org/10.1007/s10549-005-5991-z> (2005).
59. Knobel, H. *et al.* Late medical complications and fatigue in Hodgkin's disease survivors. *Journal of clinical oncology: official journal of the American Society of Clinical Oncology* **19**, 3226–3233 (2001).
60. Luctkar-Flude, M., Groll, D., Woodend, K. & Tranmer, J. Fatigue and physical activity in older patients with cancer: a six-month follow-up study. *Oncol Nurs Forum* **36**, 194–202, <https://doi.org/10.1188/09.ONF.194-202> (2009).
61. Meeske, K. *et al.* Fatigue in breast cancer survivors two to five years post diagnosis: a HEAL Study report. *Qual Life Res* **16**, 947–960, <https://doi.org/10.1007/s11136-007-9215-3> (2007).
62. Goedendorp, M. M. *et al.* Prolonged impact of chemotherapy on fatigue in breast cancer survivors: a longitudinal comparison with radiotherapy-treated breast cancer survivors and noncancer controls. *Cancer* **118**, 3833–3841, <https://doi.org/10.1002/cncr.26226> (2012).
63. Christensen, C. O., Cronin-Fenton, D., Froslev, T., Hermann, A. P. & Ewertz, M. Change in bone mineral density during adjuvant chemotherapy for early-stage breast cancer. *Supportive care in cancer: official journal of the Multinational Association of Supportive Care in Cancer*, doi:<https://doi.org/10.1007/s00520-016-3250-y> (2016).
64. Lee, S. W., Yeo, S. G., Oh, I. H., Yeo, J. H. & Park, D. C. Bone mineral density in women treated for various types of gynecological cancer. *Asia Pac J Clin Oncol*, doi:<https://doi.org/10.1111/ajco.12584> (2016).
65. Wei, R. L. *et al.* Bone mineral density loss in thoracic and lumbar vertebrae following radiation for abdominal cancers. *Radiation Oncol* **118**, 430–436, <https://doi.org/10.1016/j.radonc.2016.03.002> (2016).
66. de Gramont, A. *et al.* Randomized trial comparing monthly low-dose leucovorin and fluorouracil bolus with bimonthly high-dose leucovorin and fluorouracil bolus plus continuous infusion for advanced colorectal cancer: a French intergroup study. *Journal of clinical oncology: official journal of the American Society of Clinical Oncology* **15**, 808–815, <https://doi.org/10.1200/JCO.1997.15.2.808> (1997).
67. Douillard, J. Y. *et al.* Irinotecan combined with fluorouracil compared with fluorouracil alone as first-line treatment for metastatic colorectal cancer: a multicentre randomised trial. *Lancet* **355**, 1041–1047 (2000).
68. Tournigand, C. *et al.* FOLFIRI followed by FOLFOX6 or the reverse sequence in advanced colorectal cancer: a randomized GERCOR study. *Journal of clinical oncology: official journal of the American Society of Clinical Oncology* **22**, 229–237, <https://doi.org/10.1200/JCO.2004.05.113> (2004).
69. Kirstein, M. M. *et al.* Targeted therapies in metastatic colorectal cancer: a systematic review and assessment of currently available data. *The oncologist* **19**, 1156–1168, <https://doi.org/10.1634/theoncologist.2014-0032> (2014).
70. Mohelnikova-Duchonova, B., Melichar, B. & Soucek, P. FOLFOX/FOLFIRI pharmacogenetics: the call for a personalized approach in colorectal cancer therapy. *World J Gastroenterol* **20**, 10316–10330, <https://doi.org/10.3748/wjg.v20.i30.10316> (2014).
71. Hensing, T. A., Schell, M. J., Lee, J. H. & Socinski, M. A. Factors associated with the likelihood of receiving second line therapy for advanced non-small cell lung cancer. *Lung Cancer* **47**, 253–259, <https://doi.org/10.1016/j.lungcan.2004.07.040> (2005).
72. Jeremic, B., Milicic, B., Dagovic, A., Aleksandrovic, J. & Milisavljevic, S. Stage III non-small-cell lung cancer treated with high-dose hyperfractionated radiation therapy and concurrent low-dose daily chemotherapy with or without weekend chemotherapy: retrospective analysis of 301 patients. *Am J Clin Oncol* **27**, 350–360 (2004).
73. Huang, R. S., Kistner, E. O., Bleibel, W. K., Shukla, S. J. & Dolan, M. E. Effect of population and gender on chemotherapeutic agent-induced cytotoxicity. *Mol Cancer Ther* **6**, 31–36, <https://doi.org/10.1158/1535-7163.MCT-06-0591> (2007).
74. Fonseca, H. *et al.* Effects of doxorubicin administration on bone strength and quality in sedentary and physically active Wistar rats. *Osteoporos Int* **27**, 3465–3475, <https://doi.org/10.1007/s00198-016-3672-x> (2016).
75. Clarke, B. Normal bone anatomy and physiology. *Clin J Am Soc Nephrol* **3**(Suppl 3), S131–139, <https://doi.org/10.2215/CJN.04151206> (2008).
76. Raghu Nadhanan, R. *et al.* Dietary emu oil supplementation suppresses 5-fluorouracil chemotherapy-induced inflammation, osteoclast formation, and bone loss. *American journal of physiology. Endocrinology and metabolism* **302**, E1440–1449, <https://doi.org/10.1152/ajpendo.00587.2011> (2012).
77. Fan, C. *et al.* Combination chemotherapy with cyclophosphamide, epirubicin and 5-fluorouracil causes trabecular bone loss, bone marrow cell depletion and marrow adiposity in female rats. *J Bone Miner Metab* **34**, 277–290, <https://doi.org/10.1007/s00774-015-0679-x> (2016).
78. Murphy, K. T., Cobani, V., Ryall, J. G., Ibejunjo, C. & Lynch, G. S. Acute antibody-directed myostatin inhibition attenuates disuse muscle atrophy and weakness in mice. *Journal of applied physiology* **110**, 1065–1072, <https://doi.org/10.1152/jappphysiol.01183.2010> (2011).
79. Bialek, P. *et al.* A myostatin and activin decoy receptor enhances bone formation in mice. *Bone* **60**, 162–171, <https://doi.org/10.1016/j.bone.2013.12.002> (2014).
80. Compston, J. Emerging therapeutic concepts for muscle and bone preservation/building. *Bone* **80**, 150–156, <https://doi.org/10.1016/j.bone.2015.04.013> (2015).
81. Chow, J. W., Fox, S., Jagger, C. J. & Chambers, T. J. Role for parathyroid hormone in mechanical responsiveness of rat bone. *The American journal of physiology* **274**, E146–154 (1998).
82. Vahle, J. L. *et al.* Skeletal changes in rats given daily subcutaneous injections of recombinant human parathyroid hormone (1–34) for 2 years and relevance to human safety. *Toxicol Pathol* **30**, 312–321, <https://doi.org/10.1080/01926230252929882> (2002).

83. Jollette, J. *et al.* Comparing the incidence of bone tumors in rats chronically exposed to the selective PTH type 1 receptor agonist abaloparatide or PTH(1-34). *Regul Toxicol Pharmacol* **86**, 356–365, <https://doi.org/10.1016/j.yrtph.2017.04.001> (2017).
84. Early Breast Cancer Trialists' Collaborative, G. Adjuvant bisphosphonate treatment in early breast cancer: meta-analyses of individual patient data from randomised trials. *Lancet* **386**, 1353–1361, doi:[https://doi.org/10.1016/S0140-6736\(15\)60908-4](https://doi.org/10.1016/S0140-6736(15)60908-4) (2015).
85. O'Connell, K. E. *et al.* The effects of an ActRIIb receptor Fc fusion protein ligand trap in juvenile simian immunodeficiency virus-infected rhesus macaques. *FASEB J* **29**, 1165–1175, <https://doi.org/10.1096/fj.14-257543> (2015).
86. Bechir, N. *et al.* ActRIIB blockade increases force-generating capacity and preserves energy supply in exercising mdx mouse muscle *in vivo*. *FASEB J* **30**, 3551–3562, <https://doi.org/10.1096/fj.201600271RR> (2016).
87. Loumaye, A. *et al.* Role of Activin A and myostatin in human cancer cachexia. *The Journal of clinical endocrinology and metabolism* **100**, 2030–2038, <https://doi.org/10.1210/jc.2014-4318> (2015).
88. Chen, J. L. *et al.* Elevated expression of activins promotes muscle wasting and cachexia. *FASEB J* **28**, 1711–1723, <https://doi.org/10.1096/fj.13-245894> (2014).
89. Zimmers, T. A. *et al.* Exogenous GDF11 induces cardiac and skeletal muscle dysfunction and wasting. *Basic research in cardiology* **112**, 48, <https://doi.org/10.1007/s00395-017-0639-9> (2017).
90. Waning, D. L. *et al.* Excess TGF-beta mediates muscle weakness associated with bone metastases in mice. *Nature medicine* **21**, 1262–1271, <https://doi.org/10.1038/nm.3961> (2015).
91. Loumaye, A. *et al.* Circulating Activin A predicts survival in cancer patients. *Journal of cachexia, sarcopenia and muscle*, doi:<https://doi.org/10.1002/jcsm.12209> (2017).
92. Ding, H. *et al.* Activin A induces skeletal muscle catabolism via p38beta mitogen-activated protein kinase. *Journal of cachexia, sarcopenia and muscle* **8**, 202–212, <https://doi.org/10.1002/jcsm.12145> (2017).
93. Ogawa, Y. *et al.* Bovine bone activin enhances bone morphogenetic protein-induced ectopic bone formation. *The Journal of biological chemistry* **267**, 14233–14237 (1992).
94. Fuller, K., Bayley, K. E. & Chambers, T. J. Activin A is an essential cofactor for osteoclast induction. *Biochemical and biophysical research communications* **268**, 2–7, <https://doi.org/10.1006/bbrc.2000.2075> (2000).
95. Gaddy-Kurten, D., Coker, J. K., Abe, E., Jilka, R. L. & Manolagas, S. C. Inhibin suppresses and activin stimulates osteoblastogenesis and osteoclastogenesis in murine bone marrow cultures. *Endocrinology* **143**, 74–83, <https://doi.org/10.1210/endo.143.1.8580> (2002).
96. Goh, B. C. *et al.* Activin receptor type 2A (ACVR2A) functions directly in osteoblasts as a negative regulator of bone mass. *The Journal of biological chemistry* **292**, 13809–13822, <https://doi.org/10.1074/jbc.M117.782128> (2017).
97. Pearsall, R. S. *et al.* A soluble activin type IIA receptor induces bone formation and improves skeletal integrity. *Proceedings of the National Academy of Sciences of the United States of America* **105**, 7082–7087, <https://doi.org/10.1073/pnas.0711263105> (2008).
98. Sugatani, T. *et al.* Ligand trap of the activin receptor type IIA inhibits osteoclast stimulation of bone remodeling in diabetic mice with chronic kidney disease. *Kidney Int* **91**, 86–95, <https://doi.org/10.1016/j.kint.2016.07.039> (2017).
99. Bonetto, A. *et al.* STAT3 activation in skeletal muscle links muscle wasting and the acute phase response in cancer cachexia. *PloS one* **6**, e22538, <https://doi.org/10.1371/journal.pone.0022538> (2011).
100. Carson, J. A. & Baltgalvis, K. A. Interleukin 6 as a key regulator of muscle mass during cachexia. *Exercise and sport sciences reviews* **38**, 168–176, <https://doi.org/10.1097/JES.0b013e3181f44f11> (2010).
101. Kumar, S. *et al.* Interleukin-1 alpha promotes tumor growth and cachexia in MCF-7 xenograft model of breast cancer. *Am J Pathol* **163**, 2531–2541 (2003).
102. Costelli, P. *et al.* Tumor necrosis factor-alpha mediates changes in tissue protein turnover in a rat cancer cachexia model. *The Journal of clinical investigation* **92**, 2783–2789, <https://doi.org/10.1172/JCI116897> (1993).
103. Chen, J. L. *et al.* Differential Effects of IL6 and Activin A in the Development of Cancer-Associated Cachexia. *Cancer research* **76**, 5372–5382, <https://doi.org/10.1158/0008-5472.CAN-15-3152> (2016).
104. Trendelenburg, A. U., Meyer, A., Jacobi, C., Feige, J. N. & Glass, D. J. TAK-1/p38/nNFkappaB signaling inhibits myoblast differentiation by increasing levels of Activin A. *Skelet Muscle* **2**, 3, <https://doi.org/10.1186/2044-5040-2-3> (2012).
105. Koh, A. J., Sinder, B. P., Entezami, P., Nilsson, L. & McCauley, L. K. The skeletal impact of the chemotherapeutic agent etoposide. *Osteoporos Int* **28**, 2321–2333, <https://doi.org/10.1007/s00198-017-4032-1> (2017).
106. DiGirolamo, D. J., Kiel, D. P. & Esser, K. A. Bone and skeletal muscle: neighbors with close ties. *J Bone Miner Res* **28**, 1509–1518, <https://doi.org/10.1002/jbmr.1969> (2013).
107. Chen, Y. S. *et al.* GDF8 inhibits bone formation and promotes bone resorption in mice. *Clin Exp Pharmacol Physiol* **44**, 500–508, <https://doi.org/10.1111/1440-1681.12728> (2017).
108. Yakar, S. *et al.* Circulating levels of IGF-1 directly regulate bone growth and density. *The Journal of clinical investigation* **110**, 771–781, <https://doi.org/10.1172/JCI15463> (2002).
109. Qin, Y. *et al.* Myostatin inhibits osteoblastic differentiation by suppressing osteocyte-derived exosomal microRNA-218: A novel mechanism in muscle-bone communication. *The Journal of biological chemistry* **292**, 11021–11033, <https://doi.org/10.1074/jbc.M116.770941> (2017).
110. Sakai, R. & Eto, Y. Involvement of activin in the regulation of bone metabolism. *Mol Cell Endocrinol* **180**, 183–188 (2001).
111. Wildemann, B., Kadow-Romacker, A., Haas, N. P. & Schmidmaier, G. Quantification of various growth factors in different demineralized bone matrix preparations. *J Biomed Mater Res A* **81**, 437–442, <https://doi.org/10.1002/jbm.a.31085> (2007).
112. Waning, D. L. & Guise, T. A. Cancer-associated muscle weakness: What's bone got to do with it? *Bonekey Rep* **4**, 691, <https://doi.org/10.1038/bonekey.2015.59> (2015).
113. Hamrick, M. W. The skeletal muscle secretome: an emerging player in muscle-bone crosstalk. *Bonekey Rep* **1**, 60, <https://doi.org/10.1038/bonekey.2012.60> (2012).
114. Borsheim, E. *et al.* Pamidronate attenuates muscle loss after pediatric burn injury. *J Bone Miner Res* **29**, 1369–1372, <https://doi.org/10.1002/jbmr.2162> (2014).
115. Mera, P., Laue, K., Wei, J., Berger, J. M. & Karsenty, G. Osteocalcin is necessary and sufficient to maintain muscle mass in older mice. *Mol Metab* **5**, 1042–1047, <https://doi.org/10.1016/j.molmet.2016.07.002> (2016).
116. Karsenty, G. & Olson, E. N. Bone and Muscle Endocrine Functions: Unexpected Paradigms of Inter-organ Communication. *Cell* **164**, 1248–1256, <https://doi.org/10.1016/j.cell.2016.02.043> (2016).
117. Fontes-Oliveira, C. C. *et al.* Mitochondrial and sarcoplasmic reticulum abnormalities in cancer cachexia: altered energetic efficiency? *Biochim Biophys Acta* **1830**, 2770–2778, <https://doi.org/10.1016/j.bbagen.2012.11.009> (2013).
118. Lee, Y. S. *et al.* Muscle hypertrophy induced by myostatin inhibition accelerates degeneration in dysferlinopathy. *Hum Mol Genet* **24**, 5711–5719, <https://doi.org/10.1093/hmg/ddv288> (2015).
119. Bonetto, A., Andersson, D. C. & Waning, D. L. Assessment of muscle mass and strength in mice. *Bonekey Rep* **4**, 732, <https://doi.org/10.1038/bonekey.2015.101> (2015).
120. Schneider, C. A., Rasband, W. S. & Eliceiri, K. W. NIH Image to ImageJ: 25 years of image analysis. *Nat Methods* **9**, 671–675 (2012).
121. Bouxsein, M. L. *et al.* Guidelines for assessment of bone microstructure in rodents using micro-computed tomography. *Journal of Bone and Mineral Research* **25**, 1468–1486 (2010).

Acknowledgements

This study was supported by the National Institutes of Health (grant R21CA190028 to A.B.), the Department of Surgery and the Department of Otolaryngology – Head&Neck Surgery at Indiana University School of Medicine and by National Institutes of Health/National Institute of Aging (grant 1PO1AG039355 to L.F.B.). The authors would like to thank Dr. Se-Jin Lee (Johns Hopkins University, Baltimore, MD) for kindly providing the CHO-ACVR2B/Fc cells, Matthew Prideaux for assistance with bone samples, and John Spence for his precious contribution in editing the manuscript.

Author Contributions

R.B., L.F.B. and A.B. conceived and designed the experiments; R.B., F.P., K.C.C., K.E.C. and A.B. performed the *in vivo* experiments, the body composition assessment and the muscle function analysis; Y.K., T.M. and L.F.B. performed and analyzed the bone morphometry analysis; F.P. performed the ELISAs; T.M.O., M.E.C., L.F.B. and A.B. wrote the paper.

Additional Information

Supplementary information accompanies this paper at <https://doi.org/10.1038/s41598-017-15040-1>.

Competing Interests: The authors declare that they have no competing interests.

Publisher's note: Springer Nature remains neutral with regard to jurisdictional claims in published maps and institutional affiliations.



Open Access This article is licensed under a Creative Commons Attribution 4.0 International License, which permits use, sharing, adaptation, distribution and reproduction in any medium or format, as long as you give appropriate credit to the original author(s) and the source, provide a link to the Creative Commons license, and indicate if changes were made. The images or other third party material in this article are included in the article's Creative Commons license, unless indicated otherwise in a credit line to the material. If material is not included in the article's Creative Commons license and your intended use is not permitted by statutory regulation or exceeds the permitted use, you will need to obtain permission directly from the copyright holder. To view a copy of this license, visit <http://creativecommons.org/licenses/by/4.0/>.

© The Author(s) 2017